PROCEEDINGS OF SCIENCE

Reconstructing Air-Shower Observables using a Universality-Based Model

Maximilian Stadelmaier[a,b,c,*] **for the Pierre Auger Collaboration**

[a] *Istituto Nazionale di Fisica Nucleare, Sezione Milano, Milano, Italy*
[b] *Dipartimento di Fisica, Università degli Studi di Milano, Milano, Italy*
[c] *Institute for Astroparticle Physics, Karlsruhe Institute of Technology, Karlsruhe, Germany*
Full author list: https://www.auger.org/archive/authors_2024_11.html

E-mail: spokesperson@auger.org

Air-Shower universality describes the regularity in the longitudinal, lateral, and energy distributions of electromagnetic shower particles, as motivated by solutions of the cascade equations. To reconstruct air-shower observables from ultra-high-energy cosmic rays, we employ a universality-based model of shower development that incorporates hadronic particle components. Depending on the input parameters, the model can be used, for example, to estimate the depth of the shower maximum or the number of muons on event level. In this context, we present the expected performance for the reconstruction using air-shower simulations and data from the Pierre Auger Observatory.

7th International Symposium on Ultra High Energy Cosmic Rays (UHECR2024)
17. – 21. November 2024
Malargüe, Mendoza, Argentina

PIERRE AUGER OBSERVATORY

*Speaker

ISSN 1824-8039. Published by SISSA Medialab.

PoS(UHECR2024)117

1. Introduction

Ultra-high-energy cosmic rays (UHECRs) are the highest energy particles known to humankind; they challenge the hypothesized limits for the acceleration of particles, while a single source of UHECRs has not yet been identified [1]. Although experimental evidence implies that the spectrum of cosmic rays is strongly dominated by ionized nuclei for energies greater than 10^{18} eV (1 EeV) [2, 3], the exact chemical composition of the UHECRs is still unknown.

Due to the low flux at the highest energies, the UHECRs are not observed directly, but indirectly by the extensive air showers they induce in the Earth's atmosphere. These are cascades of secondary particles created when a UHECR interacts with an air nucleus at the top of the atmosphere. At the highest energies, the footprint of an air shower at the ground reaches several kilometers in diameter and can therefore be detected by a sparse array of surface detector stations. To estimate the chemical composition (nuclear masses) of UHECRs, a precise understanding of the air shower phenomenon is crucial. Especially the depth X_{max} of the maximum of air-shower development and the relative number of muons R_{μ} in the shower are strong indicators of the primary mass of the cosmic ray. Studies on both X_{max} and R_{μ} have been performed individually with different methods [4–6].

The largest detector for UHECRs is the Pierre Auger Observatory [7] in Malargüe, Argentina. The Observatory operates two independent detector systems, the fluorescence detector and the surface detector, which together make up a hybrid detector. The first observes the atmosphere during clear nights for fluorescence light emitted by air showers, the latter records the particle footprint at the ground at 1400 m above sea level (approximately 880 g/cm^2 vertical atmospheric mass column). The main surface detector is made up of about 1600 water-Cherenkov detectors placed in a hexagonal grid with a spacing of 1500 m. The Observatory is fully efficient to detect cosmic rays above a primary energy of 3 EeV and can be used to reconstruct various air-shower observables.

In this work, we apply a shower model to data from the Pierre Auger Observatory, with which both X_{max} and R_{μ} can be estimated.

2. A Model from Air-Shower Universality

Air-shower universality states that the electromagnetic particles in individual air showers initiated by primary particles at high primary energies E_0 show the same energy spectrum, as well as radial and angular distributions, and that these distributions and spectra are well described by idealized models such as those given in [9–11]. Especially around the maximum of the shower, where the electromagnetic particles of a shower on average carry the same energy, the longitudinal and lateral distributions of the particles (profiles), the energy spectra, and the angular distributions of particles are in a good approximation the same for all showers. This is true independent of the absolute value of X_{max} and of the type of primary particle.

Universality allows one to create an approximate model of the shower particle density in which the dependence on the distance r to the shower axis ($f(r)$), on the distance ΔX to the shower maximum ($g(\Delta X)$), and the primary energy (power law) factorizes. Thus, the shower particle footprint can be described by a function of the form

$$\varrho \simeq (E_0/E_{\mathrm{ref}})^{\gamma}\ f(r)\ g(\Delta X). \tag{1}$$

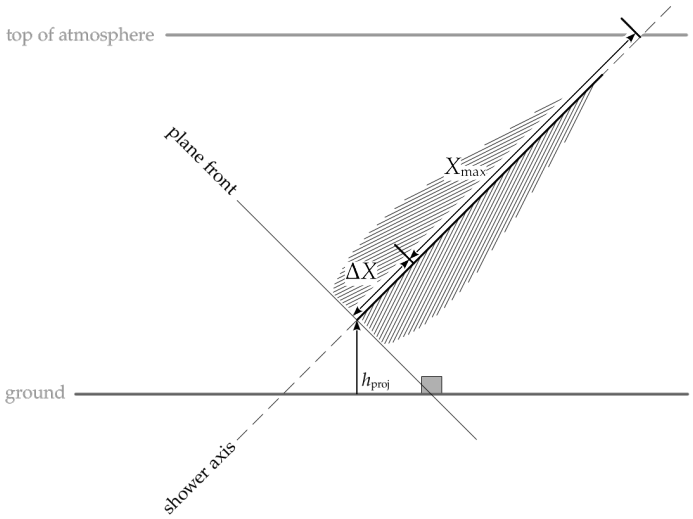

Figure 1: Sketch of the air-shower geometry, showing the distance ΔX of the station to the shower maximum at the depth $X_{\max}$, and the shower plane front as well as the shower axis. The projection height h_{proj} is given by $r \sin\theta \cos\psi$, with spherical coordinates r, θ, and ψ. See [8] for details.

A detailed description of the model used in this work and the functional forms of f and g can be found in [8]. To be able to describe not only electromagnetic but also hadronic air showers, the model of Eq. (1) is parametrized for four individual particle components in air showers, and the relative contribution R_μ of the muonic and hadronic components is kept as a free parameter. A sketch of the model behavior is given in Fig. 2.

Additionally, using the concept applied in [13] to measure the atmospheric depth of the maximum muon production, and assuming universal shower profiles, the temporal distribution of the signal in surface detector stations can be related to the depth $X_{\max}$ of the shower maximum. In this way, not only the signal footprint at the ground but also the time-dependent detector data can be used to reconstruct shower observables.

3. Hybrid Data: Number of Muons

The number of muons is a reliable proxy for the hadronic particle production in the shower development. For different primary particles, the number of muons produced per nucleus does not increase linearly with the primary energy, but approximately according to $\sim(E_0/A\,20\,\text{GeV})^\beta$, with $\beta \simeq 0.95$ [14, 15] and the atomic mass number[1] A. Thus, more muons will be produced in air showers produced by heavy nuclei, as the primary energy is distributed approximately evenly among the nucleons of the primary particle. To accurately estimate the number of shower muons from detector data, an energy estimator that is independent of the shower particle footprint can help to disentangle the apparent dependence of the number of muons and the primary energy. In this work we take use of the direct fluorescence detector measurements of the shower profile to estimate the primary energy. Using the fluorescence detector energy estimate E_0^{FD} as an input

[1] For iron nuclei relative to proton nuclei we expect an increase of a factor of $N_{\text{Fe}}/N_{\text{p}} \sim 56(1/56)^\beta \simeq 1.2$ in muons produced.

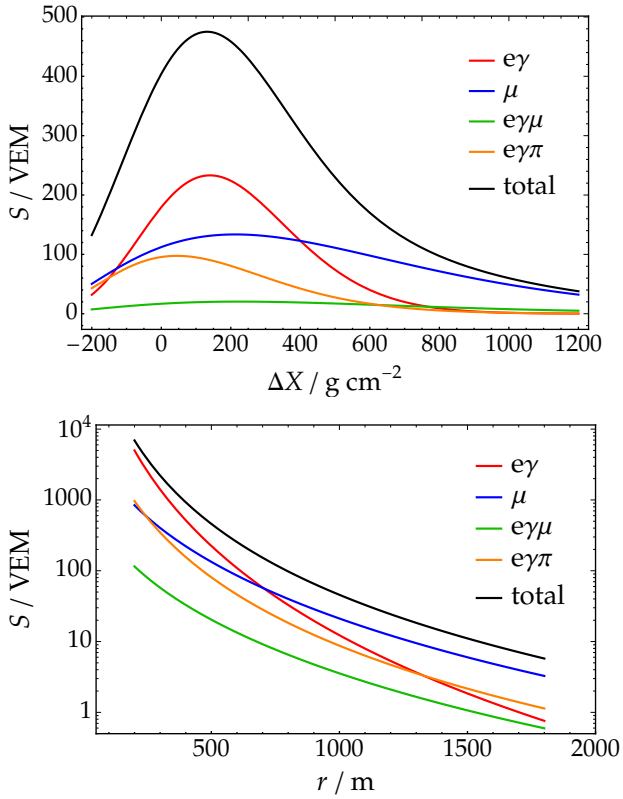

Figure 2: Sketch of the shower model described in Eq. (1). The different colors depict the contribution of four particle components to the total (black) expected signal in a detector at the distance ΔX from the shower maximum and r from the shower axis. The longitudinal development of the expected signal (*top*) is evaluated at a distance of 500 m from the shower axis; the lateral distribution of the expected signal (*bottom*) is evaluated for a shower with a zenith angle of $\theta = 12°$ and $X_{\max} = 700\,\mathrm{g/cm^2}$. The signal is given in units of VEM [12].

for the model described in Section 2, the number of muons can be accurately estimated using the surface detector measurements [16]. Therefore, to measure the number of muons we rely on *Golden Hybrid* showers. Golden Hybrid is referred to showers that are both independently reconstructable by the fluorescence and surface detectors, and that fulfill a strict set of quality criteria to ensure unbiased and precise measurements of the primary energy, the depth of the shower maximum, and the shower footprint; for details concerning the quality criteria and the reconstruction see [17, 18].

The shower footprint at the ground, which is made of the individual station signals S, is then fitted according to

$$S \simeq S_{\mathrm{e\gamma}}(E_0) + R_\mu\, S_{\mathrm{had}}(E_0), \tag{2}$$

where the electromagnetic and hadronic signal components, $S_{\mathrm{e\gamma}}$ and $S_{\mathrm{had}} = S_\mu + S_{\mathrm{e\gamma(\mu)}} + S_{\mathrm{e\gamma(\pi)}}$, are given by the shower model. The different signal contributions correspond to the particle components depicted in Fig. 2. The model signal at $R_\mu = 1$ is expected from an average proton shower as simulated with the Epos-LHC model of hadronic interactions [19].

To describe the signal at the ground level, not only the estimated primary energy, but also the direct measurement of the depth of the shower maximum from the fluorescence detector measurement is taken into account. In this way, the model is considering the effect of the individual event-level shower development on the particle footprint instead of the commonly used CIC method [20]. The performance of the fit described by Eq. (2) was evaluated using simulations; for details see [16]. In general, the number of muons can be estimated accurately independently of the type of primary particle and the zenith angle of the arrival direction; the overall precision is better than ~10% of

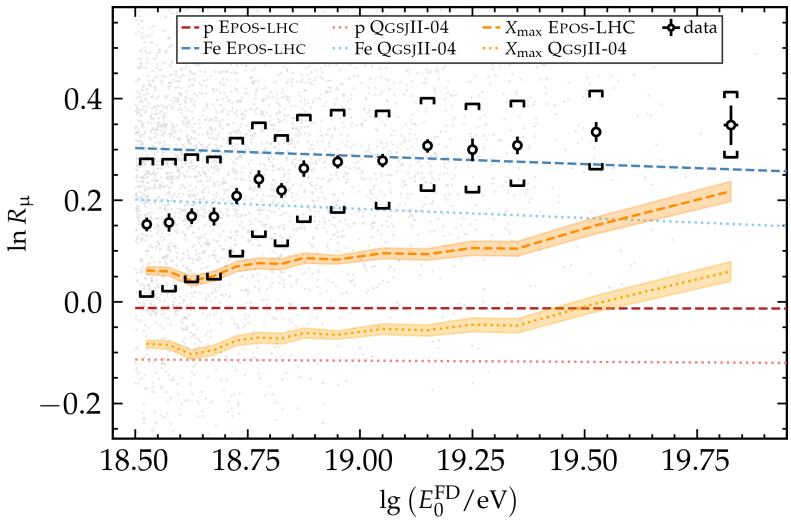

Figure 3: The relative muon number reconstructed using the universality model as a function of the primary energy measured by the fluorescence detector. The expectations from different hadronic interaction models and primary particles are given as blue and red reference lines. Expectations according to the X_{max} measurements of the showers are depicted in orange. The systematic uncertainties of the estimated number of muons are depicted as black brackets around the data points.

the total number of muons, and is thus sufficient to distinguish different types of primary particles on average. The systematic uncertainties of the estimated number of muons are dominated by the uncertainty on the fluorescence detector energy scale.

The number of muons measured with the universality model are depicted in logarithmic scale as a function of the logarithmic primary energy in Fig. 3 alongside expectations from simulated air showers using the EPOS-LHC and QGSJETII-04 [21] models of hadronic interaction. The logarithm of the muon number is expected to increase linearly with the logarithmic atomic mass number of the primary cosmic ray. The expectations for the number of muons from the measurements of the average X_{max} are substantially lower than the data. This tension is known as the well established *muon deficit* or *muon puzzle*, which is present in the data of the Pierre Auger Observatory and other air-shower experiments [5, 22].

4. Surface Detector Data: Depth of the Shower Maximum

The detector time traces (the time dependent signals) are related to the shower development in the atmosphere. This empirically confirmed connection was used already previously to infer mass-composition information from the surface detector data of the Pierre Auger Observatory [23]. In this work, the detector time traces are parametrized analytically as a function of the shower development, using the arrival time t_{pf} of the shower plane front passing through the detector as a reference. The time quantile t_{40}, at which 40% of the (total) signal have been deposited in a detector station, was found to be directly dependent on ΔX and thus on the depth of the shower maximum [8]. Note that the total signal is composed as a sum of four signal components analogously to the components depicted in Fig. 2. Using a quasi-spherical shower model, t_{40} can be expressed

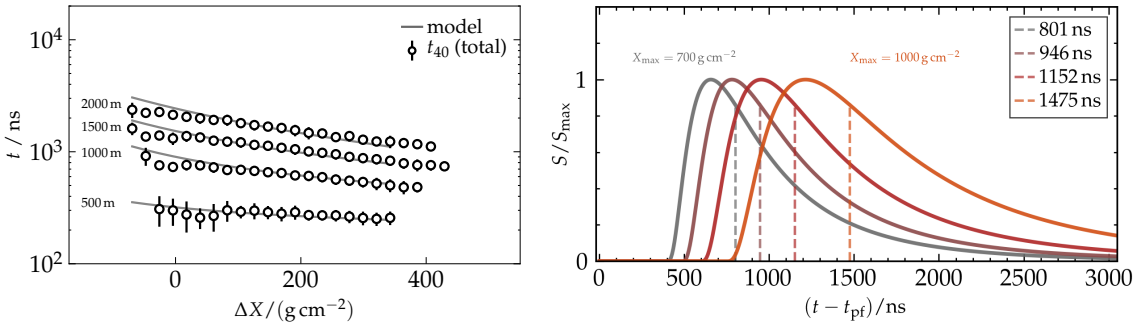

Figure 4: Left: Model and simulations for the time quantile t_{40} of the detector time traces as a function of ΔX for different distances to the shower maximum using showers at $\theta = 32°$. **Right:** Resulting normalized idealized detector time traces for a detector at a distance of 1500 m to the shower axis for four equidistant values of X_{max}. t_{40} relative to the plane-front time is indicated as a dashed line.

globally as a function of the shower geometry for each detector station at the ground; for details, see again [8]. The model for t_{40} for detector stations at different distances to the shower axis is depicted in Fig. 4 (*left*) for simulated showers at $\theta = 32°$ as a function of ΔX. Normalized idealized detector traces for a detector station at a distance of 1500 m to the shower axis are depicted in Fig. 4 (*right*) for showers with the depth of the shower maximum at 700 g/cm^2, 800 g/cm^2, 900 g/cm^2 and 1000 g/cm^2.

Using this model, we can fit the time-dependent surface detector data of the Pierre Auger Observatory to estimate the depth of the shower maximum, X_{max}. For this purpose the traces are normalized; in this way, the effect of both the number of muons and the primary energy on the X_{max}-fit is minimized. We thus expect the results to not be artificially correlated with any other observables. Stations that are far away from the shower axis ($r \geq 1800$ m) are removed from the fit, since their traces carry little to no information about the depth of the shower maximum, and the model fails to accurately describe the shower data at distances beyond $r \simeq 2000$ m, see Fig. 4 (*left*). The performance of this indirect reconstruction method to estimate X_{max} was tested both using simulations and Golden Hybrid data. For the latter, the surface detector data was analyzed independently of the fluorescence detector information and the estimated values of X_{max} were compared for each event. Fig. 5 shows the event-level comparison between directly and indirectly obtained values of X_{max}. A constant elongation rate was removed from the data[2]. Although the performance of the universality reconstruction is not *on par* with novel machine-learning methods [24–27], we observe a significant correlation for the two data sets. The universality model reconstruction is therefore fit to estimate the depth of the shower maximum from the detector time traces.

5. Discussion and Further Application

The universality shower model discussed in [8] and used in this work proves itself capable of describing and reconstruction air-shower data from the Pierre Auger Observatory. If direct information from the fluorescence detector system is used, the model can be utilized to estimate

[2] $X^{19}_{\mathrm{max}} = X_{\mathrm{max}} - D\ \lg(E_0/10^{19}\,\mathrm{eV})$ using a constant decadal elongation rate, $D \simeq 56\,\mathrm{g/cm^2}$.

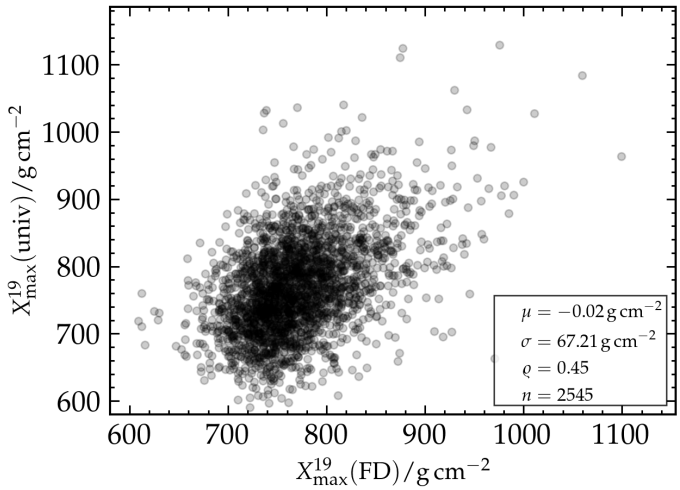

Figure 5: Correlation of the estimated (univ) and directly measured (FD) values of the depth of the shower maxima in the Golden Hybrid data set. The moments of the residual distribution as well as the Pearson correlation and the number of events is given in the legend. See the text for details.

the number of muons produced in the shower from the particle footprint information recorded by surface detector stations. The hereby obtained information about the number of muons can be used to examine the hadronic interactions in the shower, or to try and infer mass composition information directly from the muons in the shower. In combination with the event-level direct measurements of X_{max} the muon number can be used to estimate the primary mass more precisely, and to infer a model-independent width of the mass composition of the cosmic ray beam from the correlation of the two observables [16, 28].

The indirect estimation of X_{max} from the surface detector data can be used to infer mass estimation from a much larger data set, as one is not restricted to clear, moonless nights. The universality estimator therefore augments existing surface-detector based mass estimator methods [23, 29]. The obtained mass information will be used, for example, to cross-check existing methods, to investigate hadronic interactions in air showers, and to augment and amplify arrival direction data to search for possible large-scale or small-scale signals by selecting or de-selecting events based on the estimated values of X_{max} [30, 31].

References

[1] R. Alves Batista et al., *Front. Astron. Space Sci.* **6** (2019) 23 [1903.06714].
[2] Pierre Auger Collaboration, *JCAP* **10** (2019) 022 [1906.07422].
[3] Pierre Auger Collaboration, *Phys. Rev. Lett.* **125** (2020) 121106 [2008.06488].
[4] Pierre Auger Collaboration, *Phys. Rev. D* **90** (2014) 122006 [1409.5083].
[5] Pierre Auger Collaboration, *Phys. Rev. D* **91** (2015) 032003 [1408.1421].
[6] Pierre Auger Collaboration, *Phys. Rev. Lett.* **126** (2021) 152002 [2102.07797].
[7] Pierre Auger Collaboration, *Nucl. Instrum. Meth. A* **798** (2015) 172 [1502.01323].
[8] M. Stadelmaier, R. Engel, M. Roth et al., *Phys. Rev. D* **110** (2024) 023030 [2405.03494].
[9] B. Rossi and K. Greisen, *Rev. Mod. Phys.* **13** (1941) 240.
[10] J. Nishimura and K. Kamata, *Prog. Theor. Phys.* **5** (1950) 899.
[11] S. Lafebre, R. Engel, H. Falcke et al., *Astropart. Phys.* **31** (2009) 243 [0902.0548].
[12] Pierre Auger Collaboration, *Nucl. Instrum. Meth. A* **568** (2006) 839 [2102.01656].
[13] Pierre Auger Collaboration, *Phys. Rev. D* **90** (2014) 012012 [1407.5919].
[14] J. Matthews, *Astropart. Phys.* **22** (2005) 387.
[15] K.A. Cheminant et al., *PoS* **ICRC2023** (2023) 243 [2308.16525].
[16] Pierre Auger Collaboration, *PoS* **ICRC2023** (2023) 339.
[17] Pierre Auger Collaboration, *Phys. Rev. D* **90** (2014) 122005 [1409.4809].
[18] Pierre Auger Collaboration, *Phys. Rev. D* **102** (2020) 62005 [2008.06486].
[19] T. Pierog, I. Karpenko, J.M. Katzy et al., *Phys. Rev. C* **92** (2015) 034906 [1306.0121].
[20] J. Hersil, I. Escobar, D. Scott et al., *Phys. Rev. Lett.* **6** (1961) 22.
[21] S. Ostapchenko, *Phys. Rev. D* **83** (2011) 014018 [1010.1869].
[22] J.C. Arteaga Velazquez, *PoS* **ICRC2023** (2023) 466.
[23] Pierre Auger Collaboration, *Phys. Rev. D* **96** (2017) 122003 [1710.07249].
[24] Pierre Auger Collaboration, *PoS* **UHECR2024** (2024) 080.
[25] Pierre Auger Collaboration, *PoS* **ICRC2023** (2023) 371.
[26] Pierre Auger Collaboration, *Phys. Rev. Lett.* **134** (2025) 021001 [2406.06315].
[27] Pierre Auger Collaboration, *Phys. Rev. D* **111** (2025) 022003 [2406.06319].
[28] M. Stadelmaier, *Astrophys. J.* **946** (2023) 100.
[29] Pierre Auger Collaboration, *JINST* **16** (2021) P07019 [2101.02946].
[30] Pierre Auger Collaboration, *PoS* **UHECR2024** (2024) 068.
[31] Pierre Auger Collaboration, *PoS* **UHECR2024** (2024) 072.